THE JOURNAL OF BIOLOGICAL CHEMISTRY VOL. 289, NO. 14, pp. 10155–10167, April 4, 2014
Published in the U.S.A.

Myocilin Regulates Cell Proliferation and Survival*[S]

Received for publication, December 31, 2013, and in revised form, February 10, 2014 Published, JBC Papers in Press, February 22, 2014, DOI 10.1074/jbc.M113.547091

Myung Kuk Joe[‡], Heung Sun Kwon[‡], Radu Cojocaru[‡§], and Stanislav I. Tomarev[‡1]

From the [‡]Section of Retinal Ganglion Cell Biology, Laboratory of Retinal Cell and Molecular Biology, NEI, National Institutes of Health, Bethesda, Maryland 20892 and [§]Elsevier Life Science Solutions, Rockville, Maryland 20852

Background: The physiological function(s) of myocilin, a glaucoma-associated protein, is poorly understood.
Results: Myocilin enhances cell proliferation and survival together with the activation of the ERK signaling pathway. Myocilin-deficient mesenchymal stem cells demonstrate reduced proliferation and survival.
Conclusion: Myocilin participates in the regulation of cell growth and survival.
Significance: This study provides new insight into the role of myocilin in ocular and non-ocular tissues.

Myocilin, a causative gene for open angle glaucoma, encodes a secreted glycoprotein with poorly understood functions. To gain insight into its functions, we produced a stably transfected HEK293 cell line expressing myocilin under an inducible promoter and compared gene expression profiles between myocilin-expressing and vector control cell lines by a microarray analysis. A significant fraction of differentially expressed genes in myocilin-expressing cells was associated with cell growth and cell death, suggesting that myocilin may have a role in the regulation of cell growth and survival. Increased proliferation of myocilin-expressing cells was demonstrated by the WST-1 proliferation assay, direct cell counting, and immunostaining with antibodies against Ki-67, a cellular proliferation marker. Myocilin-containing conditioned medium also increased proliferation of unmodified HEK293 cells. Myocilin-expressing cells were more resistant to serum starvation-induced apoptosis than control cells. TUNEL-positive apoptotic cells were dramatically decreased, and two apoptotic marker proteins, cleaved caspase 7 and cleaved poly(ADP-ribose) polymerase, were significantly reduced in myocilin-expressing cells as compared with control cells under apoptotic conditions. In addition, myocilin-deficient mesenchymal stem cells exhibited reduced proliferation and enhanced susceptibility to serum starvation-induced apoptosis as compared with wild-type mesenchymal stem cells. Phosphorylation of ERK1/2 and its upstream kinases, c-Raf and MEK, was increased in myocilin-expressing cells compared with control cells. Elevated phosphorylation of ERK1/2 was also observed in the trabecular meshwork of transgenic mice expressing 6-fold higher levels of myocilin when compared with their wild-type littermates. These results suggest that myocilin promotes cell proliferation and resistance to apoptosis via the ERK1/2 MAPK signaling pathway.

Myocilin was discovered as one of the proteins that were induced by a long term dexamethasone treatment of cultured human trabecular meshwork cells with a time course similar to that of corticosteroid-induced glaucoma (1). For that reason, the protein was originally named TIGR (trabecular meshwork-inducible glucocorticoid response protein). Myocilin is a secreted glycoprotein that consists of 504 amino acids in humans and contains the olfactomedin domain at its C terminus (2–4). This domain is present in 13 different proteins in mammals (5). The N-terminal region of myocilin contains leucine zipper motifs within two coil-coil domains, a signal sequence, and an *N*-glycosylation site (2, 6). The leucine zipper motifs are important for oligomerization of myocilin (6–8). To date, more than 70 glaucoma-associated mutations have been identified in the myocilin (*MYOC*) gene, with the majority (>90%) of these mutations located within the third exon encoding the olfactomedin domain (5, 9–12). Mutations in *MYOC* are found in ~3–4% of all patients with primary open angle glaucoma and in more than 10% of patients with juvenile open angle glaucoma, an early onset and more severe form of glaucoma (10, 11, 13, 14).

Several lines of evidence have revealed the characteristic properties of disease-associated mutant myocilins. Mutant myocilins associated with severe forms of glaucoma are relatively insoluble in the non-ionic detergent, Triton X-100, as compared with wild-type myocilin (15). In cell cultures, mutant myocilins are not secreted from cultured cells and accumulated in the endoplasmic reticulum as insoluble aggregates, which leads to deleterious effects and cell death (16–20). Our recent report (21) demonstrated that the expression of mutated myocilins sensitizes cells to apoptosis induced by oxidative stress. In agreement with the cell culture results, mutant myocilins seem not to be secreted from the eye tissues. They are not detected in the aqueous humor of patients harboring Q368X mutation in myocilin (18) or in the aqueous humor of transgenic mice expressing human mutant Y437H myocilin (22, 23). The accumulation of mutant myocilins leads to endoplasmic reticulum stress in eye angle tissues, including the trabecular meshwork, and ultimately may result in the loss of cells within the trabecular meshwork, structural changes in the outflow pathway, and elevated intraocular pressure (13, 21, 23).

High levels of *MYOC* mRNAs are detected in the trabecular meshwork and sclera (12, 24, 25) with considerable levels also detected in other ocular and non-ocular tissues, including skeletal muscle, heart, bone marrow, and sciatic nerve (12, 26–28). Despite continuous studies for over 15 years since its discovery,

* This work was supported, in whole or in part, by the National Institutes of Health, NEI, Intramural Research Program.
[S] This article contains supplemental Table S1.
[1] To whom correspondence should be addressed: Bldg. 6, Rm. 212, 6 Center Dr., SRGCB, LRCMB, National Eye Institute, NIH, Bethesda, MD 20892. Tel.: 301-496-8524; Fax: 301-480-2610; E-mail: tomarevs@nei.nih.gov.

the physiological functions of myocilin in ocular and non-ocular tissues are poorly understood. One possible approach for elucidating the functions of myocilin is through the identification of its binding partners. We reported that myocilin may induce actin cytoskeleton reorganization through interactions with components of the Wnt signaling pathways, including several Frizzled receptors, secreted Frizzled-related proteins, and Wnt-inhibitory factor 1. These data suggest that myocilin is a modulator of the Wnt signaling (29). Additionally, several extracellular matrix proteins (24, 30–32), intracellular cytoskeleton-associated proteins (7, 32), and membrane-associated proteins (33–35) have been identified as potential myocilin-binding partners.

Here we used another approach to uncover possible myocilin functions. We compared the expression profiles of control and myocilin-expressing cells using a microarray analysis and found that myocilin expression led to changes in the expression of some genes associated with cell proliferation and survival. We showed that myocilin increased cell proliferation and survival. The activation of the extracellular signal-regulated protein kinase (ERK) signaling pathway could be involved in the observed effects. These findings provide a new direction for studies aimed at the elucidation of the physiological functions of myocilin in ocular and non-ocular tissues.

EXPERIMENTAL PROCEDURES

Cell Cultures—Vector control and myocilin-expressing cell lines were generated by transfecting the HEK293 Tet-On cell line with pTRE and pTRE-*MYOC*-FLAG, respectively (21). Tet-On stably transfected cells were maintained in Dulbecco's modified Eagle's medium (DMEM) supplemented with 10% Tet system-approved fetal bovine serum (FBS; Clontech), penicillin (100 units/ml), streptomycin (100 μg/ml), hygromycin B (200 μg/ml), and G418 (100 μg/ml) at 37 °C in a humidified atmosphere of 5% CO_2.

Mouse Mesenchymal Stem Cell (MSC) Isolation and Characterization—MSCs[2] were isolated from femoral bone marrow aspirates of C57BL/6 wild-type and *Myoc*-null mice (36) as described previously (37). In brief, 6-week-old mice were sacrificed by increasing exposure to CO_2 followed by a cervical dislocation. Cutaneous tissues were removed, and the bone marrow was aspirated from femurs by flushing them with 1–2 ml of DMEM. Mononucleated cells from the bone marrow were plated at 2×10^7 cells/100 mm^2 on plastic culture dishes in DMEM supplemented with 10% FBS, penicillin (100 units/ml), and streptomycin (100 μg/ml) at 37 °C in a humidified atmosphere of 5% CO_2. Non-adherent cells were removed after 48–72 h, and adherent cells (MSCs) were replenished with fresh medium every 2–3 days until confluent. MSCs were characterized using the mouse multipotent mesenchymal stromal cell marker antibody panel (R&D Systems). Live mouse MSCs in a single-cell suspension were blocked using 1% FBS in PBS and then stained immunocytochemically for surface markers supplied with the panel. Alexa Fluor 633-conjugated goat anti-mouse IgG (Invitrogen) were used as a secondary antibody. Negative controls included cells with a primary antibody omitted from the staining protocol. Analysis was carried out using a FACSCalibur flow cytometer (BD Biosciences).

Cell Treatments—For induction of apoptosis, confluent Tet-On stable HEK293 cells or MSCs were washed twice with serum-free DMEM and further incubated in serum-free DMEM for 72 or 120 h. MEK inhibitor U0126 (Cell Signaling Technology, Beverly, MA) was dissolved in dimethyl sulfoxide (DMSO) as a 10 mM U0126 stock solution. 10 μM U0126 was added to cell culture medium 2 h prior to the induction of myocilin expression.

Microarray Analysis—Total RNA was extracted from vector control and myocilin-expressing cell lines 48 h after induction with 1 μg/ml doxycycline (DOX) using a TRIzol reagent (Invitrogen). Ten micrograms of total RNA were used for each microarray study. Gene expression profiling was performed as a service by Expression Analysis Inc. (Durham, NC) using Human Affymetrix Gene Chip U133 Plus version 2.0 (Affymetrix Inc., Santa Clara, CA).

For statistical analysis, we used the GeneSpring GX version 10.0.3 software package (Silicon Genetics, Redwood City, CA). All data are MIAME (minimum information about a microarray experiment)-compliant. Raw data have been deposited in the GEO database with accession number GSE53985. For a background correction, normalization, and summarization of expression values, we used the robust multichip average method (38). One-way analysis of variance was used to compare gene expression -fold changes between control and myocilin-expressing cells. We found 4,343 probes with a corrected p value less than 0.05 that were differentially expressed between myocilin-expressing HEK293 and vector control HEK293 cell lines. For multiple testing correction, we used the false discovery rate method (39). We found 133 annotated probe sets (71 up and 62 down), corresponding to 111 genes that have a -fold change greater than 2. This set of genes was used for a downstream systems biology study using Ingenuity® Pathway Analysis (Ingenuity Systems, Redwood City, CA) and Pathway Studio™ (Elsevier, Inc.).

qRT-PCR—Total RNA was extracted from Tet-On stably transfected HEK293 cells using a TRIzol reagent (Invitrogen). cDNA was obtained by reverse transcription of mRNA using oligo(dT) as a primer and a SuperScript III first-strand synthesis system (Invitrogen). Forward and reverse primers used are listed in Table 3. Glyceraldehyde-3-phosphate dehydrogenase (GAPDH) was used as an internal control. Quantitative PCR was performed using a SYBR Green PCR Master Mix (ABI, Foster City, CA) and a 7900HT real-time thermocycler (ABI, Foster City, CA). To quantify the relative changes in gene expression, we used the $2^{-\Delta\Delta CT}$ method. The average C_T was calculated for the target genes and internal control (*GAPDH*), and the ΔC_T ($C_{T,\,\text{target}} - C_{T,\,\text{GAPDH}}$) values were determined. All reactions were performed using at least three independent biological samples.

WST-1 Cell Proliferation Assay—Tet-On stably transfected HEK293 cells or MSCs were plated at a concentration of 1×10^4 cells/well in 96-well plates, and Tet-On stable cells were incubated with several different concentration of DOX. After 48 h,

[2] The abbreviations used are: MSC, mesenchymal stem cell; DOX, doxycycline; qRT-PCR, quantitative RT-PCR; SNEA, subnetwork enrichment analysis algorithm; CM, conditioned medium.

10 μl of WST-1 reagent (Roche Applied Science) was added into each well, and the absorbance was measured at 450 nm after 1 h of incubation using a model 680 microplate reader (Bio-Rad).

Terminal Deoxynucleotidyl Transferase-mediated dUTP Nick-end Labeling (TUNEL) Assay—Tet-On stably transfected HEK293 cells or MSCs grown on CC2-treated 4-well glass slides (Nalge Nunc International, Naperville, IL) were fixed in 4% paraformaldehyde, and apoptotic cells were stained for TUNEL positivity using an *in situ* cell death detection kit (Roche Applied Science), following the manufacturer's instructions.

Western Blotting—Tet-On stably transfected HEK293 cells or MSCs were lysed in Mg^{2+} lysis buffer (Upstate Biotechnology, Inc., Temecula, CA) containing a protease inhibitor mixture (Roche Applied Science). Mouse iridocorneal angle tissues (the ciliary body, trabecular meshwork, and base of the iris and cornea) were dissected and homogenized in the lysis buffer (50 mM Tris, pH 7.5, 5 mM EDTA, 20 mM DTT, 0.2% SDS, 1% Triton X-100, and 1% Tween 20). After centrifugation, proteins of the soluble fractions (20 μg) were separated by 4–12% gradient NU-PAGE (Invitrogen) and transferred to a nitrocellulose membrane (Invitrogen). Membranes were preincubated in a blocking buffer (5% nonfat milk, 25 mM Tris, 150 mM NaCl, 0.05% Tween 20, pH 7.4) and then incubated in a blocking buffer overnight at 4 °C with corresponding antibodies. The antibodies used were as follows: anti-FLAG (1:2,000; Sigma), anti-cleaved caspase 7 (CP7, 1:500; Cell Signaling Technology, Beverly, MA), anti-cleaved poly(ADP-ribose) polymerase (1:500; Cell Signaling Technology), anti-phospho-c-Raf (1:500; Cell Signaling Technology), anti-phospho-MEK (1:500; Cell Signaling Technology), anti-phospho-ERK (1:500; Cell Signaling Technology), anti-ERK (1:1,000; Cell Signaling Technology), anti-myocilin (36) (1:2,000), anti-GAPDH (1:2,000; Abcam), or anti-heat-shock cognate 70 (HSC70; 1:2,000; Santa Cruz Biotechnology, Inc.). Secondary antibodies (an anti-rabbit or anti-mouse horseradish peroxidase antibody; Amersham Biosciences) were diluted 1:5,000 in a blocking buffer and incubated for 2 h at room temperature. The immunoreactive bands were developed using SuperSignal WestDura (Pierce).

Immunofluorescent Labeling—Mouse eyes were fixed in 10% neutral buffered formalin at 4 °C for 24 h before processing for paraffin embedding. Deparaffinized sections were blocked in a blocking buffer (2% normal goat serum and 0.2% Triton X-100 in PBS) for 1 h and incubated with antibody against anti-phospho-ERK (1:100; Cell Signaling Technology) in a blocking buffer for 3 h. The sections were washed three times for 10 min in PBS containing 0.01% Tween 20, followed by incubation with Alexa 488-conjugated anti-rabbit secondary antibody (Molecular Probes, Inc., Eugene, OR) for 1 h. After washing four times with PBS containing 0.01% Tween 20, the sections were further incubated with DyLight 594-labeled anti-myocilin antibody for 3 h. The sections were mounted in Vectashield mounting medium with 4′,6′-diamidino-2-phenylindole (DAPI; Vector Labs). The anti-myocilin antibody was prelabeled with fluorescent dye using DyLight 594 antibody labeling kit (Pierce) according to the manufacturer's instructions. Tet-On stably transfected HEK293 cells grown on CC2-treated 4-well glass slides (Nalge Nunc International) were fixed in 4% paraformaldehyde for 20 min. Fixed cells were blocked in a blocking buffer for 1 h and incubated with antibody against Ki-67 (Millipore) for 3 h. After washing three times, the Ki-67-positive cells were fluorescently labeled by incubation with Alexa 594-conjugated anti-rabbit secondary antibody (Molecular Probes) for 30 min. After washing four times, the samples were mounted in Vectashield mounting medium with DAPI (Vector Labs). The stained samples were examined, and fluorescent images were collected using an Axioplan-2 fluorescence microscope (Carl Zeiss).

Phospho-MAPK Antibody Array—Tet-On stably transfected HEK293 cells grown on 25T flasks were incubated with 1 μg/ml DOX for 48 h. Cells were lysed in a lysis buffer provided with the human phospho-MAPK array kit (R&D Systems). Equal amounts (200 μg) of cell lysates were added to human phospho-

TABLE 1
Ingenuity pathway analysis, top biofunctions

Top biofunctions	*p* value range	No. of genes
Diseases and disorders		
Cancer	2.94E − 08 to 3.52E − 02	44
Reproductive system disease	7.11E − 06 to 3.52E − 02	30
Gastrointestinal disease	4.83E − 05 to 2.81E − 02	18
Inflammatory disease	9.53E − 05 to 1.59E − 02	5
Respiratory disease	9.53E − 05 to 3.46E − 02	16
Molecular and cellular functions		
Cell growth and proliferation	1.01E − 04 to 3.52E − 02	27
Cell-to-cell signaling and interaction	1.31E − 04 to 3.40E − 02	13
Cell morphology	4.71E − 04 to 3.36E − 02	11
Cell death	6.95E − 04 to 3.45E − 02	23
Cellular assembly and organization	1.12E − 05 to 3.36E − 02	15

TABLE 2
Top enriched subnetworks for cellular processes

Cellular process	*p* value	Genes
Cell differentiation	8.97E − 11	*SOX3, DLL1, PLA2G4A, PGR, DAB2, IGFBP5, FBN1, CD44, SFRP1, SOSTDC1, DDIT4, DPP7, TAF7L, PTGER4, CDH11, PRKCB, STC1, KCNJ2, NBN, SLC2A3, STC2, CA2, ANXA1, CHRM3, EPHA2, ADAMTS1, NEFM, RAB27B, HOXA7, ENPEP, PRSS3, TGIF1, HHIP, JDP2, TCEAL7, CNKSR2, FSCN1, SP100 ,SOX11, SLC7A11, QKI,*LHX8*, PLXNC1, CHRDL1, PHLDA2, KBTBD10, PXDN, MAFK*
Cell survival	1.38E − 09	*DLL1, PLA2G4A, PGR, IGFBP5, FBN1, CD44, SFRP1, DDIT4, PTGER4, CDH11, PRKCB, STC1, NBN, CA2, ANXA1, CHRM3, EPHA2, ADAMTS1, JDP2, SOX11, SLC7A11, ARC, VAPA, QKI, RHBDF1, RGS17, MYOC, UPP1, EBF3, SESN2*
Cell adhesion	5.24E − 08	*DLL1, PLA2G4A, PGR, DAB2, IGFBP5, FBN1, CD44, SFRP1, PTGER4, CDH11, PRKCB, KCNJ2, ANXA1, CHRM3, EPHA2, ADAMTS1, HOXA7, FSCN1, CLDN7, MFAP2, PLXNC1, MYOC, LY6K*
Cell growth	6.86E − 08	*DLL1, PLA2G4A, PGR, DAB2, IGFBP5, FBN1, CD44, SFRP1, DDIT4, PTGER4, PRKCB, NBN, SLC2A3, STC2, CA2, ANXA1, CHRM3, EPHA2, ADAMTS1, TGIF1, JDP2, TCEAL7, GPRASP1, FSCN1, SP100, CLDN7, SOX11, SLC7A11, RHBDF1, RGS17, CARD10, PHLDA2, INHBE, EBF3, SESN2, LY6K, IGFBPL1, DIS3L2*
Epithelial to mesenchymal transition	1.16E − 07	*PGR, DAB2, IGFBP5, CD44, SFRP1, CDH11, PRKCB, NBN, STC2, ANXA1, EPHA2, HHIP, JDP2, FSCN1, ESRP1*

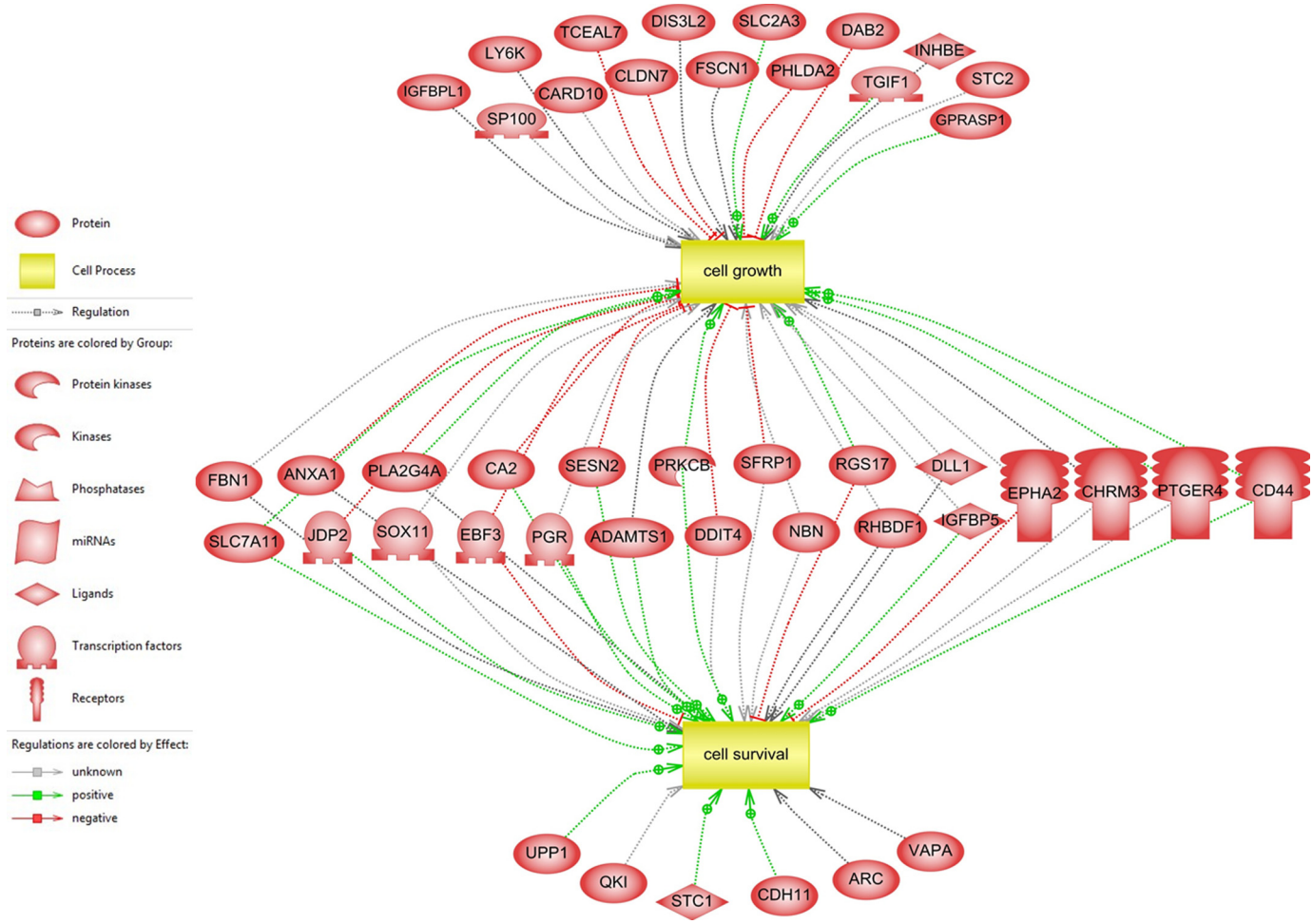

FIGURE 1. **A network of differentially expressed genes involved in cell growth and cell survival.** Subnetwork enrichment analysis identified cell growth and cell survival as significant cell processes, and the network of 44 associated genes in two cell processes was drawn by Pathway Studio. *Gray*, *green*, and *red* lines represent unknown, positive, and negative regulation, respectively.

TABLE 3
Primers used for qRT-PCR in the present study

Target gene	Gene symbol	Sequence (5′–3′)
Insulin-like growth factor binding protein-like 1	*IGFBPL1*	Forward: GGGGCCCTTCTGACCATGAG Reverse: CTGTGCTGTGGGACTCAGCC
CD44	*CD44*	Forward: CTTGCCCACAATGGCCCAGA Reverse: GGGAATCACCACGTGCCCTT
Annexin A1	*ANXA1*	Forward: GCTATCGTGAAGTGCGCCAC Reverse: GCCTTATGGCGAGTTCCAACAC
Nibrin	*NBN*	Forward: TTTTGGCTCCGGGAACGTGT Reverse: TCACCGCCAATCCAATTTCTGC
DNA damage-inducible transcript 4	*DDIT4*	Forward: AAGAACTACTGCGCCTGGCC Reverse: ACGAGGGTCAGCTGGAAGGT
Glyceraldehyde-3-phosphate dehydrogenase	*GAPDH*	Forward: GGAGTCCACTGGCGTCTTCAC Reverse: GAGGCATTGCTGATGTTGAGG

MAPK antibody arrays containing antibodies against 19 different kinases (R&D Systems). The antibody array treatment was performed according to the manufacturer's instructions. The signals were detected with SuperSignal WestDura (Pierce) by chemiluminescence. Intensities of identified spots were quantified using the ImageJ program (National Institutes of Health, Bethesda, MD).

Statistical Analysis—Data values were presented as mean ± S.D. Statistical analysis was performed using a two-tailed Student's *t* test with $p < 0.05$ being considered significant.

RESULTS

Expression Profile Analysis of Myocilin-expressing Cells—We developed a stably transfected HEK293 cell line expressing myocilin under the control of a tetracycline-inducible promoter (21). The inducibility of myocilin in this cell line was confirmed by Western blotting and qRT-PCR (see Fig. 1 in Ref. 21). To get better insight into possible functions of myocilin, we compared gene expression patterns of myocilin-expressing HEK293 and vector control HEK293 cell lines after DOX induction using Affymetrix GeneChip U133 plus 2.0 human microar-

rays. Myocilin expression induced at least 2-fold changes in the levels of 110 genes (111 including myocilin itself) that were statistically significant ($p < 0.05$) (supplemental Table S1). Next, we used the IPA software to sort differentially expressed genes into functional categories. Table 1 summarizes the top 5 biofunctions in two categories: "diseases and disorders" and "molecular and cellular functions." The IPA analysis revealed that cancer was the first biological function related to "diseases and disorders" with the highest number of genes. Fundamentally, cancer can be caused by an abnormal growth of cells. The top functions in the "molecular and cellular functions" subcategory showed that the majority of differentially expressed genes were associated with cell growth and proliferation or cell death (Table 1). These data suggested that myocilin expression may lead to changes in cell proliferation and survival.

For a systems biology approach, we used a subnetwork enrichment analysis algorithm (SNEA) using Pathway Studio software, which constructs a comprehensive collection of gene sets from ResNet, a global literature-extracted protein-protein interaction network. The gene sets are constructed for each individual network node ("seed") and consist of all of its downstream expression targets only. The central idea of the SNEA approach is that if the downstream expression targets of a seed are enriched with differentially expressed genes, then the seed is likely to be one of the key regulators of the differential expression changes (*e.g.* a transcription factor responsible for the observed changes in expression or an upstream member of the signaling pathway). In contrast to other methods that utilize the same idea of finding upstream network regulators using expression data, SNEA allows identification of any potentially important protein (not necessarily a transcriptional factor) leading to the observed expression changes, even if its own expression does not change. In this way, the two important cellular processes that we discuss in this study, cell survival and cell growth, appear on the very top with p values of 1.38E−09 and 6.86E−08, respectively (Table 2). Fig. 1 shows these two cellular processes and their connection with differentially expressed genes between myocilin-expressing HEK293 and vector control HEK293 cell lines. 44 genes among 110 differentially expressed genes were associated with cell growth or cell survival, and 23 genes were overlapped in two cellular processes (Fig. 1). To validate the results from the gene profiling experiment, we randomly selected five genes (*IGFBPL1*, *CD44*, *ANXA1*, *NBN*, and *DDIT4*) among the cell growth-associated genes and performed qRT-PCR with the specific primers (Table 3). The -fold changes in mRNA levels detected by a microarray analysis were similar to those detected by qRT-PCR, validating the accuracy of microarray data (Fig. 2). In summary, these data suggested that myocilin may be involved in cell growth and survival.

Effect of Myocilin on Cell Proliferation—Two cellular models were used to study a possible role of myocilin in the regulation of cellular proliferation and death. First, we used the stably transfected cell Tet-On HEK293 lines described above. Myocilin was not detected in a vector control line in the absence or presence of DOX (not shown). In a myocilin-expressing cell line, myocilin was not detected in the absence of DOX, but the protein levels increased with increasing DOX concentrations.

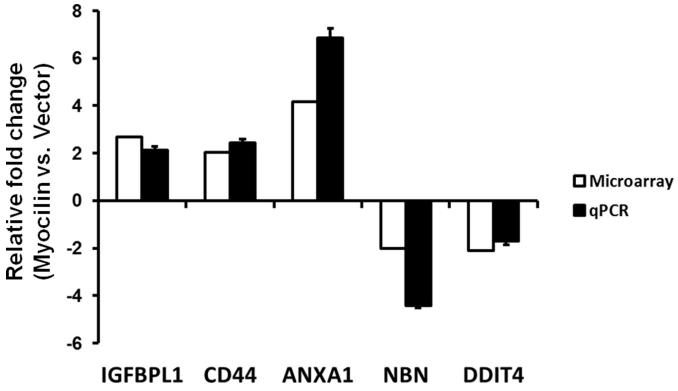

FIGURE 2. **Validation of microarray data by qRT-PCR.** Five genes involved in cell proliferation were selected from the microarray data. Changes in the levels of mRNAs in myocilin-expressing cells (*Myocilin*) *versus* vector control cells (*Vector*) as detected by microarray analysis (*white bars*) were compared with those detected by qRT-PCR (*black bars*). -Fold changes are shown on the *y* axis. Positive values represent up-regulation, and negative values represent down-regulation in HEK293 Tet-On cells following myocilin expression. Three independent biological samples were analyzed. *Error bars*, S.D.

Myocilin was detected in the conditioned medium (CM), but there was no detectable myocilin in the cell lysates (Fig. 3*A*).

Cell proliferation was first tested using the WST-1 proliferation assay. It showed the increased cell proliferation with increased concentration of DOX in myocilin-expressing cells. A maximal increase in the cell proliferation was observed at 1 μg/ml DOX. Conversely, proliferation of the vector control cell line was not significantly altered by the DOX treatment, indicating that DOX had no effect on the cell proliferation (Fig. 3*B*). These results were confirmed through comparisons of the actual cell numbers of myocilin-expressing and vector control cells. The cell number was increased by 43.0 ± 11.7% in myocilin-expressing cells relative to vector control cells after treatment with 1 μg/ml DOX for 48 h (Fig. 3*C*). The fraction of proliferative cells was assessed using immunostaining with antibodies against Ki-67. Ki-67 is a reliable proliferation marker, which is present only during active phases of the cell cycle (40). Ki-67-positive HEK293 cells showed strong and relatively weak signals, probably reflecting the fact that positive cells were in different phases of the cell cycle (Fig. 3*D*). In the $G_1/S/G_2$ phases, cells have weak punctate Ki-67 signals, whereas mitotic cells show concentrated strong signals in the nucleus (41). The amount of strongly positive Ki-67 cells representing mitotic cells was increased by 50.3 ± 4.7% ($p = 0.005$) in myocilin-expressing cells *versus* vector control cells, confirming that the former were proliferating more actively than the later (Fig. 3*D*).

Because myocilin was efficiently secreted from HEK293 cells (Fig. 3*A*), we examined whether extracellular myocilin alone may stimulate cell proliferation. We used 10-fold diluted CM from control or myocilin-expressing cells to treat non-modified HEK293 cells. The addition of myocilin-containing CM stimulated cell growth, as demonstrated by the WST-1 assay (Fig. 4*A*). This stimulatory effect of myocilin was eliminated by preincubation of CM with anti-myocilin antibodies but not with an unrelated control IgG fraction (Fig. 4*A*). The stimulatory effect of myocilin on cell proliferation was confirmed by direct cell counting. Similar to the results of the WST-1 assay, myocilin-

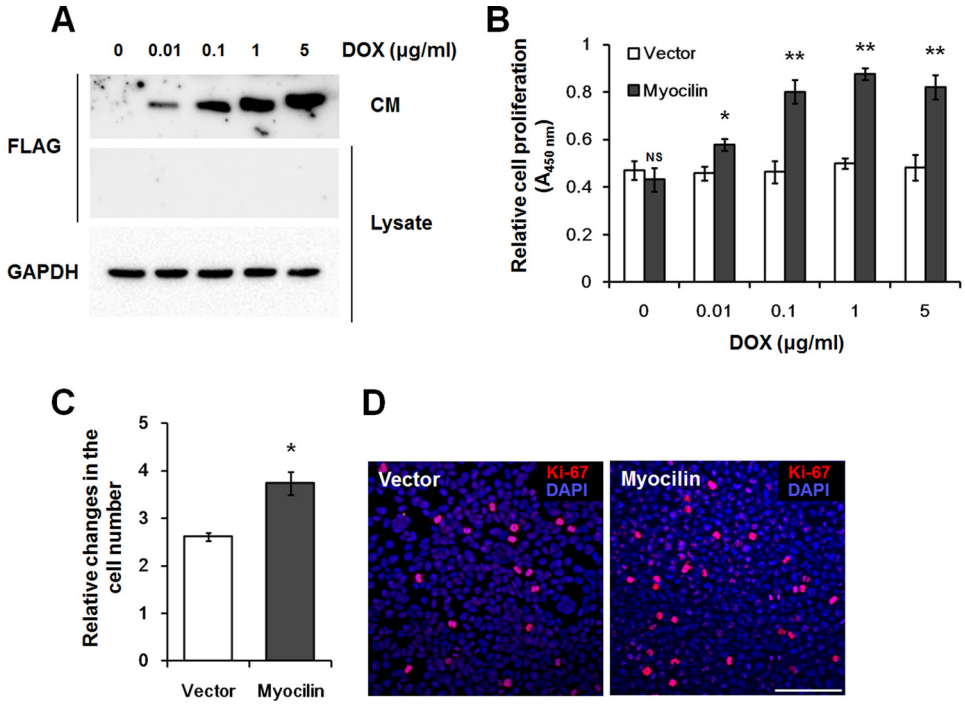

FIGURE 3. **Myocilin stimulates division of Tet-On HEK293 cells.** *A*, Western blot analysis of myocilin in CM and cell lysates. Myocilin expression was induced by the addition of indicated concentration of DOX for 48 h. Anti-FLAG antibodies were used for detection of myocilin. Staining of the same blot with antibodies against GAPDH was used for normalization of loading. *B*, WST-1 proliferation assay. Increasing DOX concentrations were added to control (*Vector*) and myocilin-expressing Tet-On HEK293 cells for 48 h. The WST-1 reagent was added to each well. After 1 h, the absorbance at 450 nm was measured to evaluate cell proliferation. *C*, relative changes in the cell number after incubation of control and myocilin-expressing cells in the presence of 1 μg/ml DOX for 48 h. The equal numbers of cells (1×10^5 cells/well) were plated into 6-well plates, and the increased numbers of cells were calculated as -fold changes relative to initial plating numbers. *Error bars*, S.D. of triplicate cultures. *D*, immunostaining of control and myocilin-expressing Tet-On HEK 293 cells with Ki-67 antibodies. Cells were plated in triplicate cultures and grown for 48 h in the presence of 1 μg/ml DOX. Nuclei were stained with DAPI. *Scale bar*, 100 μm (*NS*, non-significant; *, $p < 0.05$; **, $p < 0.01$).

containing medium increased the number of cells by about 25% after 2 days in culture, and this stimulatory effect was reduced by the addition of anti-myocilin antibodies but not a control IgG fraction (Fig. 4*B*). We concluded that extracellular myocilin may stimulate cell proliferation.

Protective Effect of Myocilin against Serum Starvation-induced Apoptosis—The cell proliferation-promoting properties of myocilin resemble the activities of some growth factors. A number of growth factors have been shown to regulate not only cell proliferation but also apoptotic pathways (42, 43). To assess whether myocilin affects apoptosis, control and myocilin-expressing cells were cultivated in conditions stimulating apoptosis. Cells were first treated with DOX for 24 h and then serum-starved for 72 h. Apoptotic cells were detected using a TUNEL assay. TUNEL-positive cells were significantly reduced in myocilin-expressing cells as compared with control cells (Fig. 5*A*). Additionally, two apoptotic markers, cleaved caspase 7 and cleaved poly(ADP-ribose) polymerase, were markedly decreased in myocilin-expressing cells after DOX stimulation as compared with unstimulated cells. DOX addition did not lead to changes in the levels of these two apoptotic markers in the control cell line (Fig. 5*B*). Together, these results suggest that myocilin protects cells against apoptosis.

Proliferation and Survival of Myocilin-defective MSCs—Previously, we demonstrated that myocilin is expressed in undifferentiated human and mouse MSCs (44). MSC lines are among the few cell lines that express myocilin. To test whether elimination of myocilin affects MSC proliferation or survival, we isolated MSCs from the bone marrow of wild-type and *Myoc*-null mice. Flow cytometric analysis demonstrated expression of Sca-1, CD106, CD73, CD29, and CD44 but not CD45 or CD11b in both wild-type and *Myoc*-null MSCs (Fig. 6). As expected, myocilin was detected in MSC lysates from wild-type but not from *Myoc*-null mice (Fig. 7*A*). Analysis of their proliferation rate demonstrated that *Myoc*-null MSCs have a lower proliferation rate as compared with MSCs isolated from wild-type littermates as judged by both the WST-1 proliferation assay (Fig. 7*B*) and cell counting (Fig. 7*C*). The cell number of *Myoc*-null MSCs was reduced by about 20% compared with wild-type control MSCs after 48 h of incubation (Fig. 7*C*).

Myocilin depletion also led to an increased sensitivity of MSCs to the apoptotic condition. After 5 days of serum starvation, the number of TUNEL-positive cells was significantly increased in the *Myoc*-null MSCs compared with wild-type control MSCs. The ratio of apoptotic cells was 20.2 $\pm$ 2.4% in wild-type control MSCs and 51.4 $\pm$ 5.3% in the *Myoc*-null MSCs (Fig. 7*D*). Moreover, two apoptotic markers, cleaved caspase 7 and poly(ADP-ribose) polymerase, were only detected in *Myoc*-null and not wild-type MSCs (Fig. 7*E*).

Activation of ERK Signaling Pathways by Myocilin—Cell proliferation and survival are regulated by various intracellular signaling pathways. It is well known that mitogen-activated protein kinase (MAPK) cascades are key signaling pathways involved in the regulation of cell proliferation, survival, and differentiation (45, 46). Therefore, we used a human phospho-MAPK array to test the effects of myocilin on these signaling

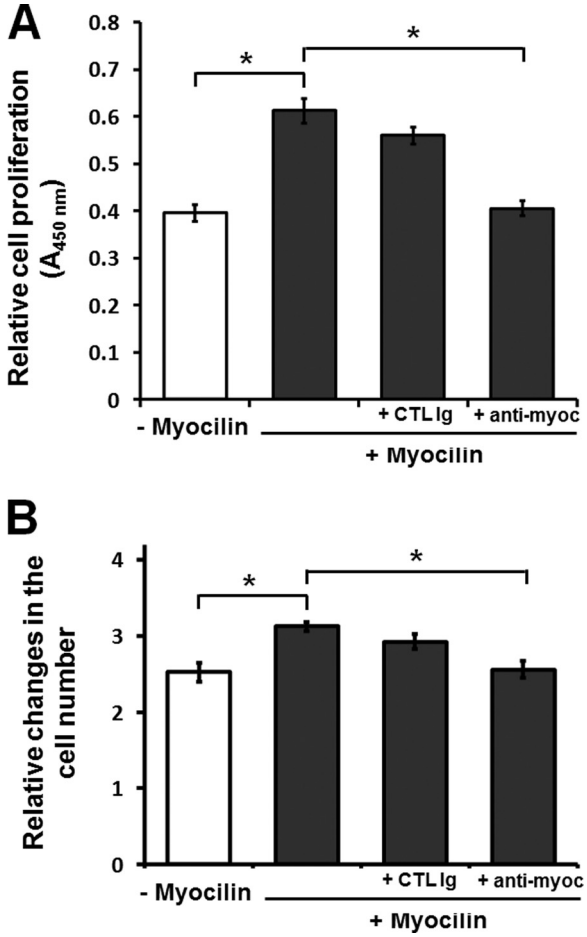

FIGURE 4. **Effects of extracellular myocilin on cell proliferation.** *A*, the WST-1 proliferation assay. HEK293 cells were treated with CM from Tet-On cells expressing (+ *Myocilin*) or non-expressing (− *Myocilin*) myocilin and tested by the WST-1 proliferation assay after 48 h. To deplete myocilin in CM, it was preincubated with monoclonal anti-myocilin antibodies (5 μg/ml) for 2 h. As a control, CM was preincubated with mouse control immunoglobulin for 2 h. *B*, 1×10^5 cells/well were incubated as in *A* and counted after 48 h (*, $p < 0.05$). *Error bars*, S.D. of triplicate cultures.

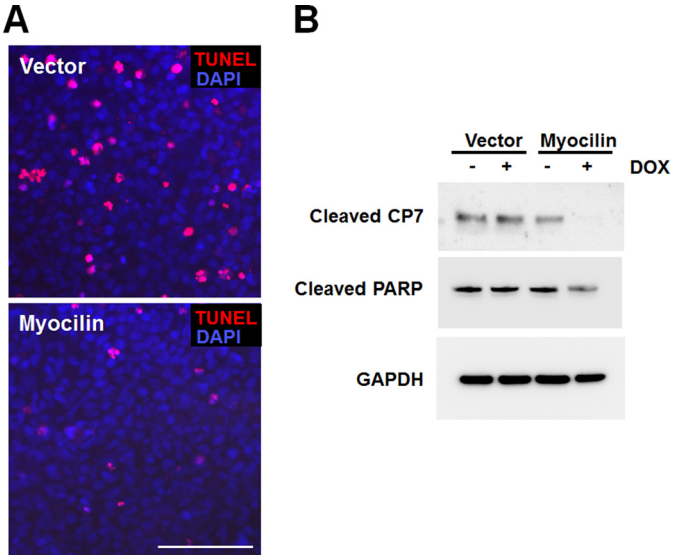

FIGURE 5. **Myocilin protects cell from serum deprivation-induced apoptosis.** *A*, control and myocilin-expressing Tet-On HEK293 cells were preincubated with 1 μg/ml DOX for 24 h and then further incubated in serum-free medium containing 1 μg/ml DOX for 72 h. Apoptotic cells (*red fluorescence*) were identified by a TUNEL assay. *Scale bar*, 100 μm. *B*, Western blot analysis of cell lysates using antibodies against cleaved CP7, cleaved poly(ADP-ribose) polymerase, and GAPDH. Cells were incubated as in *A*. Similar results were obtained in three independent experiments. Representative blots are shown.

pathways. The array included the major MAPK families (ERK, p38, and JNK) and intracellular kinases (Akt, GSK-3b, and p70 S6), which are important in the signal transduction of cell proliferation and survival. Phospho-MAPK membranes were incubated with lysates of myocilin-expressing or control HEK293 cells. The comparison of two membranes showed that phospho-ERK1/2 levels were elevated in lysate of myocilin-expressing cells (Fig. 8*A*). These data were confirmed by Western blotting analyses. A detectable level of myocilin was identified in myocilin-expressing cells 12 h after the addition of 1 μg/ml DOX (data not shown). Phospho-ERK1 and phospho-ERK2 were significantly increased at this time point (Fig. 8*B*). Quantitatively, phospho-ERK1/2 was increased by 3.1 ± 0.5 fold 12 h after induction. Longer expression of myocilin led to an additional increase of phospho-ERK1/2 (Fig. 8*C*). Moreover, ERK upstream kinases, phospho-MEK and c-Raf, were also increased after myocilin induction (Fig. 8*B*). These results suggest that the Raf-MEK-ERK MAPK cascade was activated by myocilin. Generally, the ERK pathway is activated by growth factors and critically involved in the regulation of cell proliferation and survival (45). Thus, the increased ERK signaling that we observed may contribute to the increased proliferation and survival of myocilin-expressing cells. To determine whether ERK signaling is important for myocilin function, we investigated the effects of an ERK pathway inhibitor on myocilin-induced cell proliferation and survival. U0126 is a highly selective inhibitor of both MEK1 and MEK2 kinases, both of which lie upstream of ERK1/2 in the signaling pathways (47). Pretreatment of HEK293 cells with U0126 for 2 h reduced the level of phospho-ERK and almost completely blocked the ERK activation induced by myocilin (Fig. 9*A*). In the absence of U0126, the number of cells was increased by ~30% in the myocilin-expressing conditions as compared with uninduced conditions. The difference in the cell number between the induced and uninduced lines narrowed to 6% when pretreatment with U0126 was administered (Fig. 9*B*). Additionally, the effects of myocilin on serum starvation-induced apoptosis almost disappeared in the presence of U0126. In the absence of U0126, the amount of TUNEL-positive cells was significantly reduced in myocilin-expressing cells. However, the U0126 treatment led to an increased sensitivity of the cells to the serum depletion, and the difference in the number of TUNEL-positive cells between the two groups nearly disappeared (Fig. 9*C*). Although we cannot exclude the off-target effect of U0126, our data suggest that the ERK signaling plays a significant part in myocilin-mediated increased cell proliferation and survival.

Increased ERK Activation in the Eye Angle Tissues of Myoc-transgenic Mice—To see whether myocilin may activate the ERK signaling *in vivo*, we analyzed the eye angle tissues of myocilin-overexpressing transgenic and wild-type mice. These transgenic mice had been produced previously using artificial bacterial chromosome DNA containing the full-length mouse *Myoc* gene and its long flanking sequences (48). The eye angle tissue of transgenic mice contained about 6 times more myoci-

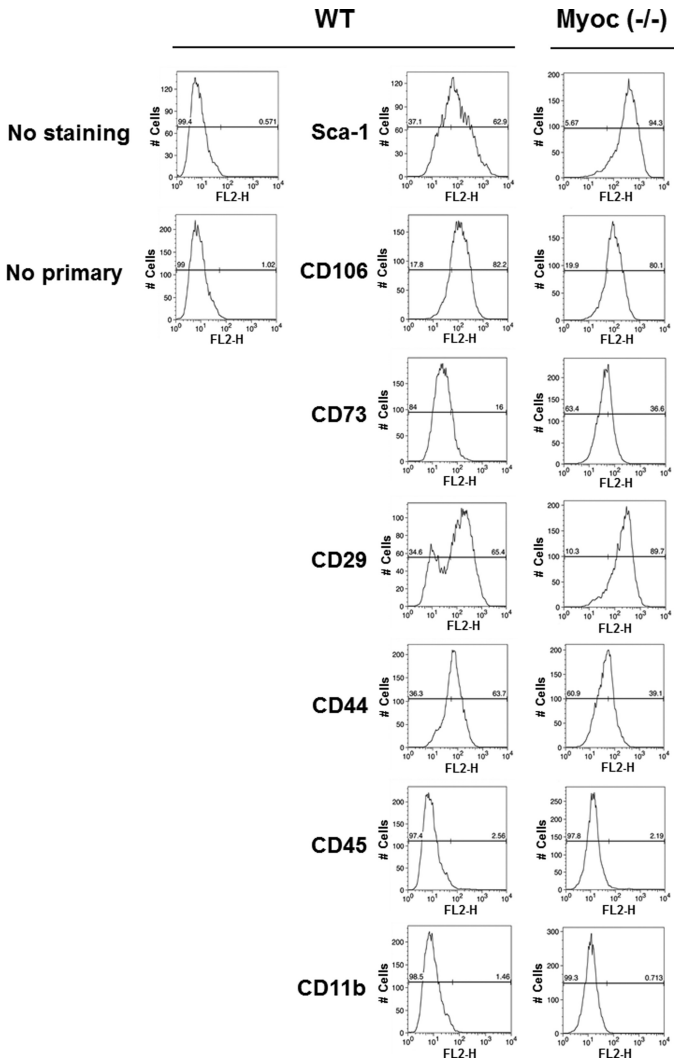

FIGURE 6. **Characterization of wild-type and *Myoc*-null mice MSCs identities by analysis of MSC marker expression.** Mouse MSCs were stained with the indicated primary antibodies supplied with the mouse multipotent mesenchymal stromal cell marker antibody panel (R&D Systems). MSCs were stained with a phycoerythrin-conjugated goat anti-rat secondary antibody and analyzed by flow cytometry. Wild-type (*middle panels*) and *Myoc*-null (*right panels*) cells demonstrate the expected phenotype for mouse MSCs (positive expression of Sca-1, CD106, CD73, CD29, and CD44; negative expression of CD45 and CD11b). The *left panels* correspond to unstained MSCs (*top*) and staining with anti-rat secondary antibody (*bottom*), respectively.

lin than that of their wild-type littermates (48). Phospho-ERK and its upstream kinase, phospho-MEK, were significantly increased in the eye angle tissues of transgenic mice (Fig. 10*A*). Quantitatively, phospho-ERK1/2 was increased by 2.7 ± 0.4-fold in the eye angle tissues of transgenic mice as compared with their wild-type littermates (Fig. 10*B*). Similarly, immunostaining of the eye sections showed a significant increase of phospho-ERK immunofluorescent signal in the trabecular meshwork area of transgenic mice compared with their wild-type littermates (Fig. 10*C*). A smaller increase of the myocilin and phospho-ERK immunofluorescent signals was also observed in the ciliary body of transgenic mice as compared with their wild-type littermates (Fig. 10*C*). We concluded that myocilin may regulate the ERK signaling pathway and its upstream kinase, phospho-MEK, *in vivo*.

DISCUSSION

The *MYOC* gene and encoded protein have been the subject of intensive investigation since the seminal 1997 discovery demonstrating the relationship between mutations in *MYOC* and glaucoma (11, 12). Available data suggest that accumulation of mutant myocilin leads to endoplasmic reticulum stress in the eye angle tissues, including the trabecular meshwork; stimulates the unfolded protein response; and ultimately leads to the loss of cells within the trabecular meshwork, resulting in structural changes in the outflow pathway and elevated intraocular pressure (13, 21, 23). Relatively few studies have described possible physiological functions of wild-type myocilin. Our recent data suggest that myocilin may have distinct extracellular and intracellular functions. Extracellular myocilin may serve as a modulator of Wnt signaling by interacting with several components of the Wnt signaling pathway (29). It may also increase cell migration by acting through the integrin-focal adhesion kinase signaling pathway (49). We showed that myocilin is expressed in MSCs, and the addition of extracellular myocilin enhances osteogenic MSC differentiation (44). Moreover, although *Myoc*-null mice do not develop glaucoma and at the first glance appeared to be normal (36), more careful analysis demonstrated that cortical bone thickness and trabecular volume, as well as the expression level of osteopontin, a known factor of bone remodeling and osteoblast differentiation, were dramatically reduced in the femurs of *Myoc*-null mice compared with wild-type mice (44). Although myocilin is secreted from several cell lines *in vitro* (18, 21) and from some tissues *in vivo* (18, 22), it is not secreted from some cell lines (*e.g.* from differentiated myotubes) (33). Intracellular myocilin may be a regulator of laminin pathways via interactions with components of the dystrophin-associated protein complex (33). Finally, our recent data suggest that myocilin plays a role in myelination of the sciatic nerve in the peripheral nervous system and optic nerve in the central nervous system (50). Here, we report another novel function of myocilin: a regulation of cell proliferation and survival.

Cell proliferation and survival are tightly regulated by a mediation of several intracellular signaling pathways. Our study supports the possibility that myocilin activates the ERK signaling pathway to promote cell proliferation and survival. The role of the ERK signaling pathway in cell proliferation and survival is well established (45, 51). Mitogenesis in cultured cell lines correlates with ERK activation, and inhibition of the ERK pathway results in reduced proliferation in most instances (52). ERK activation requires the sequential phosphorylation of c-Raf and MEK. Activation of the Raf/MEK/ERK signaling cascade is under the regulation of several growth-responsive proteins (52, 53). Growth factors like epidermal growth factor (EGF), fibroblast growth factor, and platelet-derived growth factor were originally identified as potent activators of ERK (52). In the current study, we demonstrated that myocilin is very efficiently secreted from HEK293 cells, and that secreted myocilin stimulates cell proliferation. Secreted myocilin may activate specific receptors that can control the ERK signaling cascade in a manner sim-

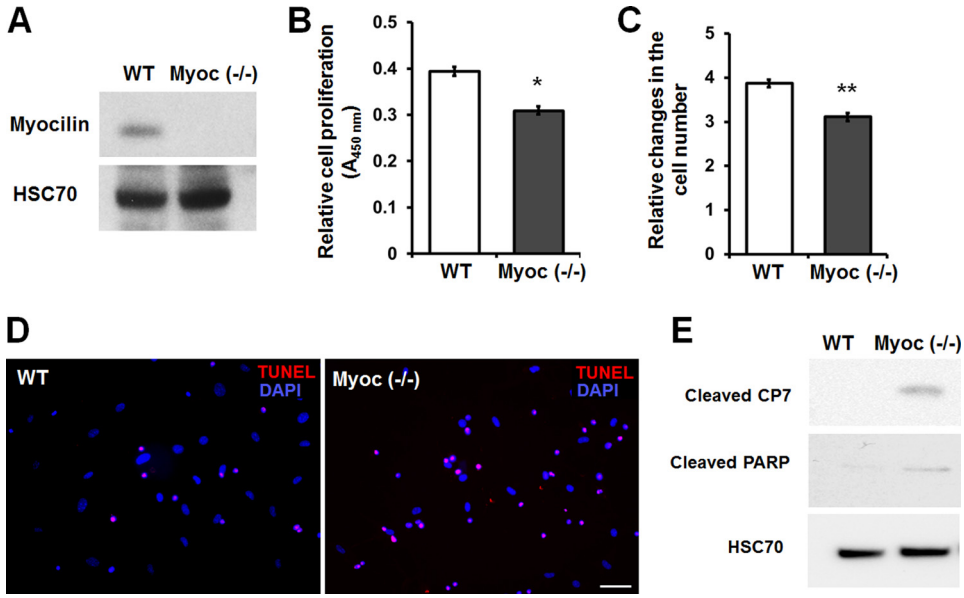

FIGURE 7. ***Myoc*-null MSCs exhibit reduced cell proliferation and increased sensitivity to serum deprivation-induced apoptosis.** *A*, Western blot analysis of MSCs isolated from wild-type or *Myoc*-null mice. Cell lysates were immunoblotted with anti-myocilin and anti-HSC70 antibodies. HSC70 was used for normalization of loading. *B*, WST-1 proliferation assay. Wild-type and *Myoc*-null MSCs were incubated for 48 h. *Error bars*, S.D. of triplicate cultures. *C*, relative changes in the cell number after incubation of wild-type and *Myoc*-null MSCs for 48 h. Equal numbers of cells (7×10^4 cells/well) were plated into 6-well plates, and changes in the number of cells were calculated as -fold changes relative to the initial plating numbers. *Error bars*, S.D. of triplicate cultures. *D*, apoptosis in wild-type and *Myoc*-null MSC cultures after incubation in serum-free medium for 120 h. Apoptotic cells (red fluorescence) were identified by TUNEL assay. *Scale bar*, 100 μm. *E*, Western blot analysis of cell lysates using antibodies against cleaved CP7, cleaved poly(ADP-ribose) polymerase, and HSC70. Cells were incubated as in *D*. Similar results were obtained in three independent experiments. Representative blots are shown. *, $p < 0.05$; **, $p < 0.01$.

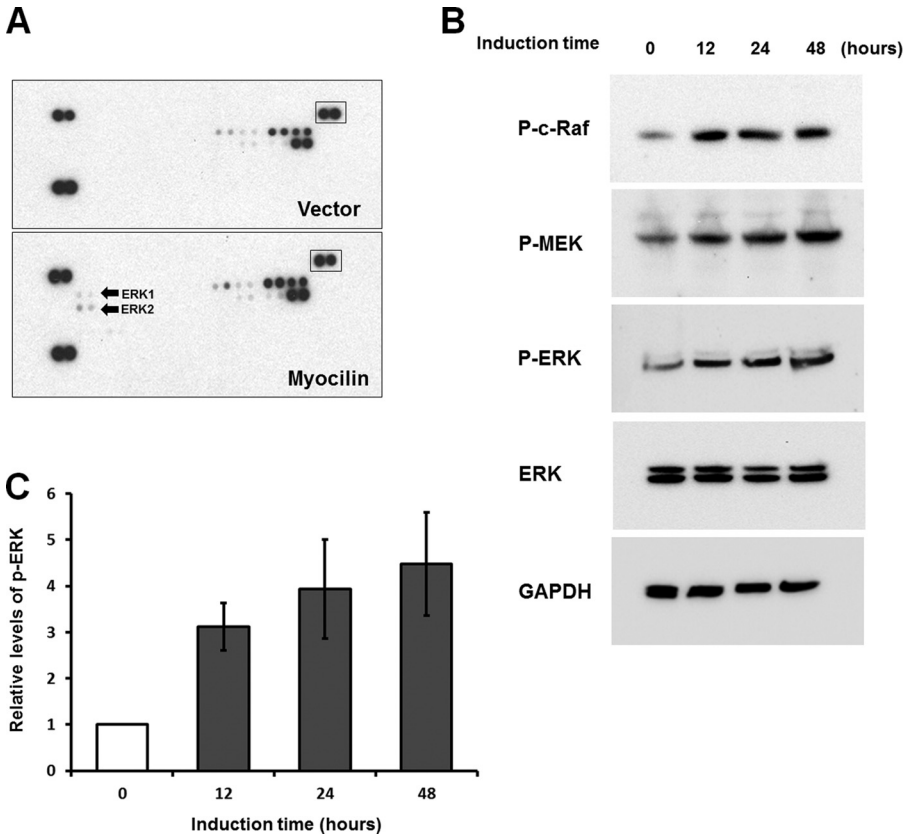

FIGURE 8. **Analysis of MAPK phosphorylation.** *A*, control and myocilin-expressing Tet-On HEK293 cells were treated with 1 μg/ml DOX for 48 h. Lysates of control (*top*) and myocilin-expressing cells (*bottom*) were added to human phospho-MAPK antibody arrays. Arrays were treated as described under "Experimental Procedures." *Arrows*, spots corresponding to phosphorylated ERK1 and ERK2 on the blots. *Boxed spots* were used for normalization. *B*, Western blot analysis of myocilin-expressing Tet-On HEK 293 cells. Cells were treated with 1 μg/ml DOX for the indicated periods of time. Cell lysates were immunoblotted with anti-phospho-c-Raf (*P-c-Raf*; 1:500 dilution), anti-phospho-MEK (*P-MEK*; 1:500 dilution), anti-phospho-ERK (*P-ERK*; 1:500 dilution), anti-total ERK (1:1,000 dilution), and anti-GAPDH (1:2,000 dilution) antibodies. *C*, quantification of the results of three independent experiments as in *B* for phospho-ERK1/2. *Error bars*, S.D.

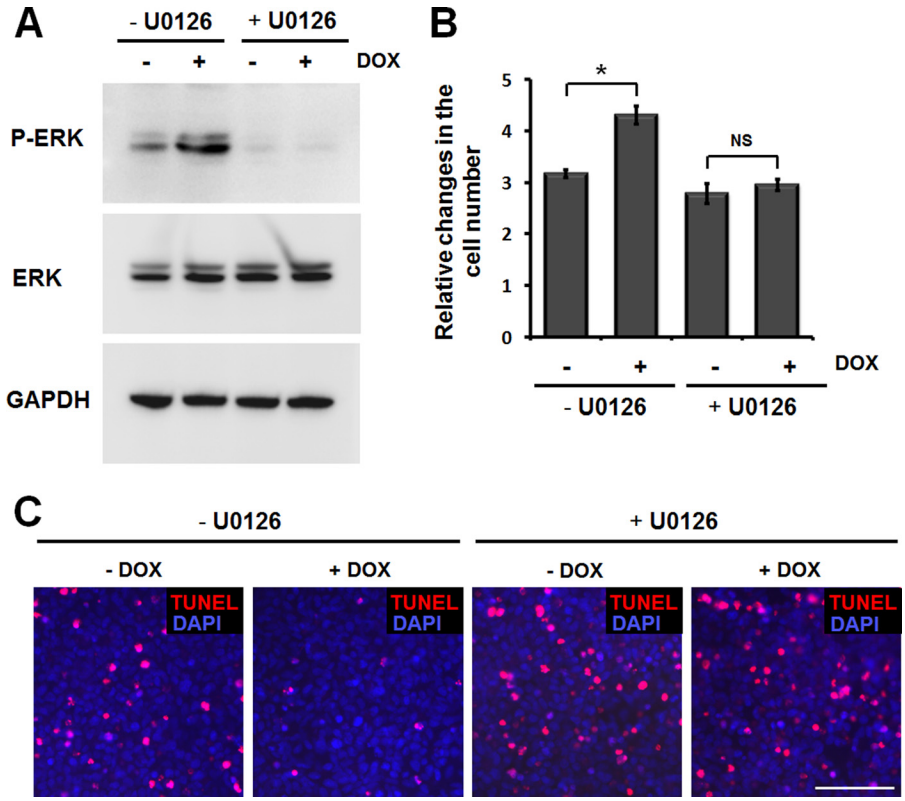

FIGURE 9. **Inhibition of ERK activation abrogates myocilin effects on cell proliferation and survival.** *A*, myocilin-expressing Tet-On HEK293 cells were pretreated with 10 μM U0126 or DMSO for 2 h and further incubated in the medium containing or lacking 1 μg/ml DOX for 48 h. Cell lysates were immunoblotted with anti-phospho-ERK (*P-ERK*; 1:500 dilution), total ERK (1:1,000 dilution), and anti-GAPDH (1:2,000 dilution) antibodies. *B*, equal numbers of cells (1×10^5 cells/well) were plated into 6-well plates and incubated as in *A*. Relative changes in the cell number after incubation in the indicated conditions are shown. *Error bars*, S.D. of triplicate cultures. *NS*, non-significant; *, $p < 0.05$. *C*, Tet-On HEK293 cells were pretreated with 10 μM U0126 or DMSO for 2 h and then incubated in the medium containing or lacking 1 μg/ml DOX for 24 h. Thereafter, the cells were further incubated in serum-free medium containing 1 μg/ml DOX for 72 h. Apoptotic cells (*red fluorescence*) were identified as by the TUNEL assay. Similar results were obtained in three independent experiments. The results of a typical experiment are shown. *Scale bar*, 100 μm.

ilar to growth factors. It is well known that the MEK/ERK-dependent survival pathway can be induced by the activation of EGF receptor (51, 52). In our previous study, we demonstrated that EGF receptor phosphorylation was enhanced by treatment with a myocilin-containing medium (50). Myocilin may also activate focal adhesion kinase and its downstream phosphatidylinositide 3-kinase (PI3K) signaling pathway (49). Focal adhesion kinase-mediated activation of the PI3K pathway is able to stimulate the Raf/MEK/ERK signaling cascade via activation of p21-activated protein kinases (54, 55). Therefore, we speculate that activation of EGF receptor and the PI3K pathway by myocilin may contribute to the activation of the MEK/ERK signaling cascade.

Increased ERK activation and cell survival induced by myocilin may have biologically important roles. The highest level of myocilin expression is observed in the trabecular meshwork, which is responsible for the regulation of aqueous humor outflow. Several lines of evidence have shown that the outflow facility can be regulated by the composition of the extracellular matrix in the trabecular meshwork. Moreover, increases in extracellular matrix materials have been associated with the development of primary open angle glaucoma and steroid-induced glaucoma (56–58). The ERK pathway plays a central role in receptor-mediated secretion of extracellular matrix proteins and matrix metalloproteinases (59–61). Additionally, our study suggests the possibility that increased activation of the ERK pathway by myocilin may increase the ability of trabecular meshwork cells to survive. The number of trabecular meshwork cells decreases with aging, and this decrease in cell number can be a cause of structural changes in the outflow pathway of aqueous humor, thereby increasing the risk of glaucoma (13, 62). Generally, normal cells require growth factors to maintain their viability (43). An abundance of myocilin in eye angle tissues may contribute to the survival of trabecular meshwork cells and other tissues in the anterior chamber of the eye. Consequently, myocilin may be involved in regulating trabecular function by activating the ERK pathway.

Our recent study demonstrated myocilin expression in human and rodent MSCs (63). Although most MSCs undergo a limited number of replications, they can replenish themselves through symmetric and asymmetric cell divisions (64). In addition, the proliferation rate of MSCs is somewhat higher than for most normal cell types. To regulate cell proliferation and survival, MSCs secrete a broad spectrum of growth factors and cytokines (65, 66). We have now demonstrated that myocilin depletion in mouse MSCs can be a cause of retarded proliferation and hypersensitivity to apoptotic treatment, suggesting that myocilin may contribute to the survival and proliferation of MSCs. Myocilin expression also has been detected in a few stem cells, including hair follicle stem cells (67, 68). Similarly,

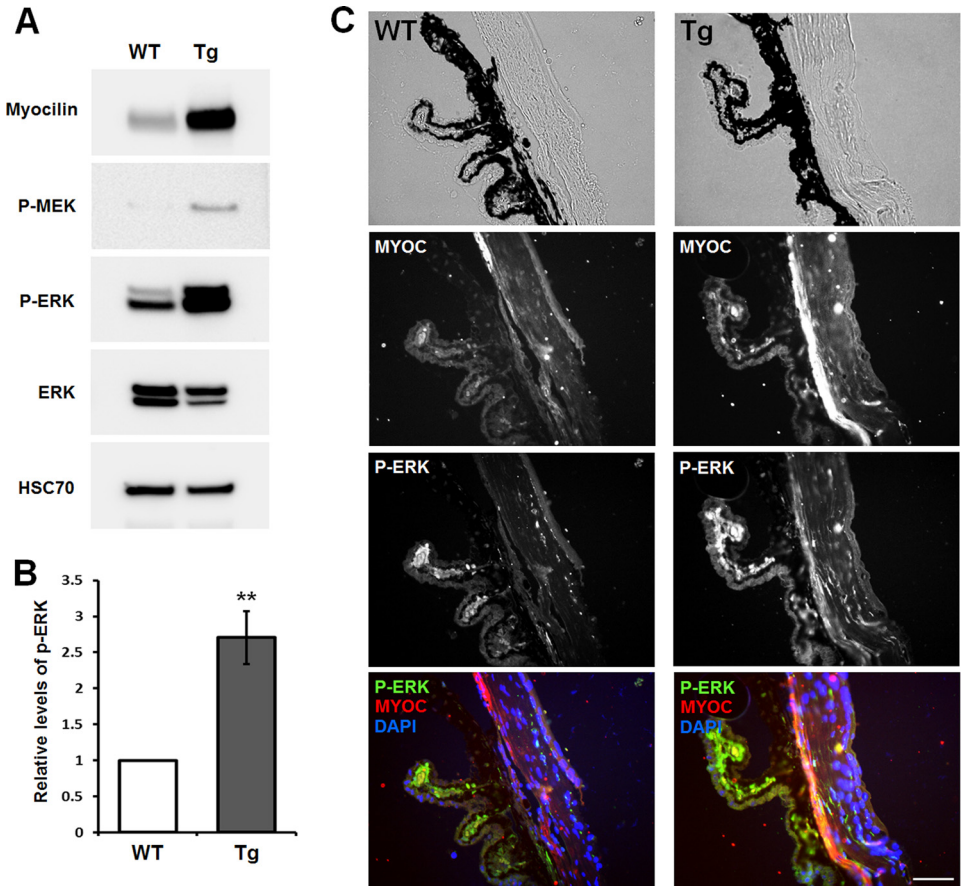

FIGURE 10. **Enhanced ERK activation in the trabecular meshwork of myocilin-expressing transgenic mice.** *A*, Western blot analysis of the indicated proteins in the eye angle tissues. Lysates from the dissected angle tissues of 8-month-old wild-type or transgenic mice were immunoblotted with anti-myocilin (1:2,000 dilution), anti-phospho-MEK (*P-MEK*; 1:500 dilution), anti-phospho-ERK (*P-ERK*; 1:500 dilution), anti-total ERK (1:1,000 dilution), and anti-HSC70 (1:2,000 dilution) antibodies. *B*, quantification of the results obtained with four pairs of mice for phospho-ERK1/2. *Error bars*, S.D. *C*, eye sections of 8-month-old wild-type and transgenic mice were stained with anti-phospho-ERK (1:100 dilution), anti-myocilin (1:100 dilution) antibody, and DAPI. *Top row*, bright field images. *TM*, trabecular meshwork; *CB*, ciliary body. *Scale bar*, 50 μm.

myocilin may play some role in a stem cell's capacity for long term self-renewal.

Recent reports demonstrate that another olfactomedin family protein, olfactomedin 4, is a robust marker for stem cells in human intestine (69, 70). It has antiapoptotic effects and promotes the proliferation of cells in a way that is similar to the effects of myocilin (71, 72). Olfactomedin 4 is also expressed at high levels in several types of cancer, like carcinomas of the breast (73), colon (70, 71, 73), stomach (71, 74), lung (73), pancreas (73), and head and neck squamous cell carcinoma (75). It may be associated with the differentiation and progression of cancer. It has been also reported that inhibition of olfactomedin-like 3 in tumor endothelial cells and pericytes efficiently reduces tumor angiogenesis and growth *in vivo* (76). Although myocilin expression has not yet been characterized in cancer cells, if myocilin expression is induced during cancer progression, it may have effects on malignancy or resistance to anticancer treatment in some cancers. Analysis of myocilin expression and its functions in cancer cells and cancer stem cells deserves further investigation.

In summary, our data demonstrate a novel function of myocilin as a regulator of the ERK pathway that is important for cell growth and survival. They imply that myocilin may have functions not only in cells of the eye but also in adult stem cells outside of the eye.

Acknowledgments—We thank Dr. Thomas V. Johnson for critical reading of the manuscript and Rafael Villasmil for help with flow cytometry analysis of MSCs. Dr. Radu Cojocaru thanks Dr. Anand Swaroop for support.

REFERENCES

1. Polansky, J. R., Fauss, D. J., Chen, P., Chen, H., Lütjen-Drecoll, E., Johnson, D., Kurtz, R. M., Ma, Z. D., Bloom, E., and Nguyen, T. D. (1997) Cellular pharmacology and molecular biology of the trabecular meshwork inducible glucocorticoid response gene product. *Ophthalmologica.* **211,** 126–139
2. Kubota, R., Noda, S., Wang, Y., Minoshima, S., Asakawa, S., Kudoh, J., Mashima, Y., Oguchi, Y., and Shimizu, N. (1997) A novel myosin-like protein (myocilin) expressed in the connecting cilium of the photoreceptor. Molecular cloning, tissue expression, and chromosomal mapping. *Genomics* **41,** 360–369
3. Ortego, J., Escribano, J., and Coca-Prados, M. (1997) Cloning and characterization of subtracted cDNAs from a human ciliary body library encoding TIGR, a protein involved in juvenile open angle glaucoma with homology to myosin and olfactomedin. *FEBS Lett.* **413,** 349–353
4. Tamm, E. R. (2002) Myocilin and glaucoma: facts and ideas. *Prog. Retin. Eye Res.* **21,** 395–428

5. Tomarev, S. I., and Nakaya, N. (2009) Olfactomedin domain-containing proteins. Possible mechanisms of action and functions in normal development and pathology. *Mol. Neurobiol.* **40,** 122–138
6. Nguyen, T. D., Chen, P., Huang, W. D., Chen, H., Johnson, D., and Polansky, J. R. (1998) Gene structure and properties of TIGR, an olfactomedin-related glycoprotein cloned from glucocorticoid-induced trabecular meshwork cells. *J. Biol. Chem.* **273,** 6341–6350
7. Wentz-Hunter, K., Ueda, J., and Yue, B. Y. (2002) Protein interactions with myocilin. *Invest. Ophthalmol. Vis. Sci.* **43,** 176–182
8. Fautsch, M. P., and Johnson, D. H. (2001) Characterization of myocilin-myocilin interactions. *Invest. Ophthalmol. Vis. Sci.* **42,** 2324–2331
9. Gong, G., Kosoko-Lasaki, O., Haynatzki, G. R., and Wilson, M. R. (2004) Genetic dissection of myocilin glaucoma. *Hum. Mol. Genet.* **13,** R91–R102
10. Fingert, J. H., Héon, E., Liebmann, J. M., Yamamoto, T., Craig, J. E., Rait, J., Kawase, K., Hoh, S. T., Buys, Y. M., Dickinson, J., Hockey, R. R., Williams-Lyn, D., Trope, G., Kitazawa, Y., Ritch, R., Mackey, D. A., Alward, W. L., Sheffield, V. C., and Stone, E. M. (1999) Analysis of myocilin mutations in 1703 glaucoma patients from five different populations. *Hum. Mol. Genet.* **8,** 899–905
11. Stone, E. M., Fingert, J. H., Alward, W. L., Nguyen, T. D., Polansky, J. R., Sunden, S. L., Nishimura, D., Clark, A. F., Nystuen, A., Nichols, B. E., Mackey, D. A., Ritch, R., Kalenak, J. W., Craven, E. R., and Sheffield, V. C. (1997) Identification of a gene that causes primary open angle glaucoma. *Science* **275,** 668–670
12. Adam, M. F., Belmouden, A., Binisti, P., Brézin, A. P., Valtot, F., Béchetoille, A., Dascotte, J. C., Copin, B., Gomez, L., Chaventré, A., Bach, J. F., and Garchon, H. J. (1997) Recurrent mutations in a single exon encoding the evolutionarily conserved olfactomedin-homology domain of TIGR in familial open-angle glaucoma. *Hum. Mol. Genet.* **6,** 2091–2097
13. Kwon, Y. H., Fingert, J. H., Kuehn, M. H., and Alward, W. L. (2009) Primary open-angle glaucoma. *N. Engl. J. Med.* **360,** 1113–1124
14. Alward, W. L., Fingert, J. H., Coote, M. A., Johnson, A. T., Lerner, S. F., Junqua, D., Durcan, F. J., McCartney, P. J., Mackey, D. A., Sheffield, V. C., and Stone, E. M. (1998) Clinical features associated with mutations in the chromosome 1 open-angle glaucoma gene (GLC1A). *N. Engl. J. Med.* **338,** 1022–1027
15. Zhou, Z., and Vollrath, D. (1999) A cellular assay distinguishes normal and mutant TIGR/myocilin protein. *Hum. Mol. Genet.* **8,** 2221–2228
16. Joe, M. K., Sohn, S., Hur, W., Moon, Y., Choi, Y. R., and Kee, C. (2003) Accumulation of mutant myocilins in ER leads to ER stress and potential cytotoxicity in human trabecular meshwork cells. *Biochem. Biophys. Res. Commun.* **312,** 592–600
17. Liu, Y., and Vollrath, D. (2004) Reversal of mutant myocilin non-secretion and cell killing: implications for glaucoma. *Hum. Mol. Genet.* **13,** 1193–1204
18. Jacobson, N., Andrews, M., Shepard, A. R., Nishimura, D., Searby, C., Fingert, J. H., Hageman, G., Mullins, R., Davidson, B. L., Kwon, Y. H., Alward, W. L., Stone, E. M., Clark, A. F., and Sheffield, V. C. (2001) Non-secretion of mutant proteins of the glaucoma gene myocilin in cultured trabecular meshwork cells and in aqueous humor. *Hum. Mol. Genet.* **10,** 117–125
19. Malyukova, I., Lee, H. S., Fariss, R. N., and Tomarev, S. I. (2006) Mutated mouse and human myocilins have similar properties and do not block general secretory pathway. *Invest. Ophthalmol. Vis. Sci.* **47,** 206–212
20. Gobeil, S., Rodrigue, M. A., Moisan, S., Nguyen, T. D., Polansky, J. R., Morissette, J., and Raymond, V. (2004) Intracellular sequestration of hetero-oligomers formed by wild-type and glaucoma-causing myocilin mutants. *Invest. Ophthalmol. Vis. Sci.* **45,** 3560–3567
21. Joe, M. K., and Tomarev, S. I. (2010) Expression of myocilin mutants sensitizes cells to oxidative stress-induced apoptosis: implication for glaucoma pathogenesis. *Am. J. Pathol.* **176,** 2880–2890
22. Zhou, Y., Grinchuk, O., and Tomarev, S. I. (2008) Transgenic mice expressing the Tyr437His mutant of human myocilin protein develop glaucoma. *Invest. Ophthalmol. Vis. Sci.* **49,** 1932–1939
23. Zode, G. S., Kuehn, M. H., Nishimura, D. Y., Searby, C. C., Mohan, K., Grozdanic, S. D., Bugge, K., Anderson, M. G., Clark, A. F., Stone, E. M., and Sheffield, V. C. (2011) Reduction of ER stress via a chemical chaperone prevents disease phenotypes in a mouse model of primary open angle glaucoma. *J. Clin. Invest.* **121,** 3542–3553
24. Torrado, M., Trivedi, R., Zinovieva, R., Karavanova, I., and Tomarev, S. I. (2002) Optimedin: a novel olfactomedin-related protein that interacts with myocilin. *Hum. Mol. Genet.* **11,** 1291–1301
25. Tomarev, S. I., Wistow, G., Raymond, V., Dubois, S., and Malyukova, I. (2003) Gene expression profile of the human trabecular meshwork: NEIBank sequence tag analysis. *Invest. Ophthalmol. Vis. Sci.* **44,** 2588–2596
26. Fingert, J. H., Ying, L., Swiderski, R. E., Nystuen, A. M., Arbour, N. C., Alward, W. L., Sheffield, V. C., and Stone, E. M. (1998) Characterization and comparison of the human and mouse GLC1A glaucoma genes. *Genome Res.* **8,** 377–384
27. Tomarev, S. I., Tamm, E. R., and Chang, B. (1998) Characterization of the mouse Myoc/Tigr gene. *Biochem. Biophys. Res. Commun.* **245,** 887–893
28. Ohlmann, A., Goldwich, A., Flügel-Koch, C., Fuchs, A. V., Schwager, K., and Tamm, E. R. (2003) Secreted glycoprotein myocilin is a component of the myelin sheath in peripheral nerves. *Glia* **43,** 128–140
29. Kwon, H. S., Lee, H. S., Ji, Y., Rubin, J. S., and Tomarev, S. I. (2009) Myocilin is a modulator of Wnt signaling. *Mol. Cell. Biol.* **29,** 2139–2154
30. Aroca-Aguilar, J. D., Sánchez-Sanchez, F., Ghosh, S., Fernández-Navarro, A., Coca-Prados, M., and Escribano, J. (2011) Interaction of recombinant myocilin with the matricellular protein SPARC: functional implications. *Invest. Ophthalmol. Vis. Sci.* **52,** 179–189
31. Ueda, J., Wentz-Hunter, K., and Yue, B. Y. (2002) Distribution of myocilin and extracellular matrix components in the juxtacanalicular tissue of human eyes. *Invest. Ophthalmol. Vis. Sci.* **43,** 1068–1076
32. Fautsch, M. P., Vrabel, A. M., and Johnson, D. H. (2006) The identification of myocilin-associated proteins in the human trabecular meshwork. *Exp. Eye Res.* **82,** 1046–1052
33. Joe, M. K., Kee, C., and Tomarev, S. I. (2012) Myocilin interacts with syntrophins and is member of dystrophin-associated protein complex. *J. Biol. Chem.* **287,** 13216–13227
34. Dismuke, W. M., McKay, B. S., and Stamer, W. D. (2012) Myocilin, a component of a membrane-associated protein complex driven by a homologous Q-SNARE domain. *Biochemistry* **51,** 3606–3613
35. Joe, M. K., Sohn, S., Choi, Y. R., Park, H., and Kee, C. (2005) Identification of flotillin-1 as a protein interacting with myocilin: implications for the pathogenesis of primary open-angle glaucoma. *Biochem. Biophys. Res. Commun.* **336,** 1201–1206
36. Kim, B. S., Savinova, O. V., Reedy, M. V., Martin, J., Lun, Y., Gan, L., Smith, R. S., Tomarev, S. I., John, S. W., and Johnson, R. L. (2001) Targeted disruption of the myocilin gene (Myoc) suggests that human glaucoma-causing mutations are gain of function. *Mol. Cell. Biol.* **21,** 7707–7713
37. Soleimani, M., and Nadri, S. (2009) A protocol for isolation and culture of mesenchymal stem cells from mouse bone marrow. *Nat. Protoc.* **4,** 102–106
38. Irizarry, R. A., Hobbs, B., Collin, F., Beazer-Barclay, Y. D., Antonellis, K. J., Scherf, U., and Speed, T. P. (2003) Exploration, normalization, and summaries of high density oligonucleotide array probe level data. *Biostatistics* **4,** 249–264
39. Benjamini, Y., and Hochberg, Y. (1995) Controlling the false discovery rate: a practical and powerful approach for multiple testing. *J. R. Stat. Soc. Ser. B* **57,** 289–300
40. Gerdes, J., Lemke, H., Baisch, H., Wacker, H. H., Schwab, U., and Stein, H. (1984) Cell cycle analysis of a cell proliferation-associated human nuclear antigen defined by the monoclonal antibody Ki-67. *J. Immunol.* **133,** 1710–1715
41. Starborg, M., Gell, K., Brundell, E., and Hoog, C. (1996) The murine Ki-67 cell proliferation antigen accumulates in the nucleolar and heterochromatic regions of interphase cells and at the periphery of the mitotic chromosomes in a process essential for cell cycle progression. *J. Cell Sci.* **109,** 143–153
42. Conlon, I., and Raff, M. (1999) Size control in animal development. *Cell* **96,** 235–244
43. Raff, M. C. (1992) Social controls on cell survival and cell death. *Nature* **356,** 397–400
44. Kwon, H. S., Johnson, T. V., and Tomarev, S. I. (2013) Myocilin stimulates osteogenic differentiation of mesenchymal stem cells through MAPK sig-

naling. *J. Biol. Chem.* **288,** 16882–16894
45. McCubrey, J. A., Steelman, L. S., Chappell, W. H., Abrams, S. L., Wong, E. W., Chang, F., Lehmann, B., Terrian, D. M., Milella, M., Tafuri, A., Stivala, F., Libra, M., Basecke, J., Evangelisti, C., Martelli, A. M., and Franklin, R. A. (2007) Roles of the Raf/MEK/ERK pathway in cell growth, malignant transformation and drug resistance. *Biochim. Biophys. Acta* **1773,** 1263–1284
46. Wada, T., and Penninger, J. M. (2004) Mitogen-activated protein kinases in apoptosis regulation. *Oncogene* **23,** 2838–2849
47. Favata, M. F., Horiuchi, K. Y., Manos, E. J., Daulerio, A. J., Stradley, D. A., Feeser, W. S., Van Dyk, D. E., Pitts, W. J., Earl, R. A., Hobbs, F., Copeland, R. A., Magolda, R. L., Scherle, P. A., and Trzaskos, J. M. (1998) Identification of a novel inhibitor of mitogen-activated protein kinase kinase. *J. Biol. Chem.* **273,** 18623–18632
48. Gould, D. B., Miceli-Libby, L., Savinova, O. V., Torrado, M., Tomarev, S. I., Smith, R. S., and John, S. W. (2004) Genetically increasing Myoc expression supports a necessary pathologic role of abnormal proteins in glaucoma. *Mol. Cell. Biol.* **24,** 9019–9025
49. Kwon, H. S., and Tomarev, S. I. (2011) Myocilin, a glaucoma-associated protein, promotes cell migration through activation of integrin-focal adhesion kinase-serine/threonine kinase signaling pathway. *J. Cell Physiol.* **226,** 3392–3402
50. Kwon, H. S., Johnson, T. V., Joe, M. K., Abu-Asab, M., Zhang, J., Chan, C. C., and Tomarev, S. I. (2013) Myocilin mediates myelination in the peripheral nervous system through ErbB2/3 signaling. *J. Biol. Chem.* **288,** 26357–26371
51. Chambard, J. C., Lefloch, R., Pouysségur, J., and Lenormand, P. (2007) ERK implication in cell cycle regulation. *Biochim. Biophys. Acta* **1773,** 1299–1310
52. Roberts, P. J., and Der, C. J. (2007) Targeting the Raf-MEK-ERK mitogen-activated protein kinase cascade for the treatment of cancer. *Oncogene* **26,** 3291–3310
53. Marshall, C. J. (1995) Specificity of receptor tyrosine kinase signaling: transient *versus* sustained extracellular signal-regulated kinase activation. *Cell* **80,** 179–185
54. Eblen, S. T., Slack, J. K., Weber, M. J., and Catling, A. D. (2002) Rac-PAK signaling stimulates extracellular signal-regulated kinase (ERK) activation by regulating formation of MEK1-ERK complexes. *Mol. Cell. Biol.* **22,** 6023–6033
55. Giancotti, F. G., and Ruoslahti, E. (1999) Integrin signaling. *Science* **285,** 1028–1032
56. Wordinger, R. J., and Clark, A. F. (1999) Effects of glucocorticoids on the trabecular meshwork: towards a better understanding of glaucoma. *Prog. Retin. Eye Res.* **18,** 629–667
57. Knepper, P. A., Goossens, W., Hvizd, M., and Palmberg, P. F. (1996) Glycosaminoglycans of the human trabecular meshwork in primary open-angle glaucoma. *Invest. Ophthalmol. Vis. Sci.* **37,** 1360–1367
58. Lütjen-Drecoll, E., Futa, R., and Rohen, J. W. (1981) Ultrahistochemical studies on tangential sections of the trabecular meshwork in normal and glaucomatous eyes. *Invest. Ophthalmol. Vis. Sci.* **21,** 563–573
59. Kurata, H., Thant, A. A., Matsuo, S., Senga, T., Okazaki, K., Hotta, N., and Hamaguchi, M. (2000) Constitutive activation of MAP kinase kinase (MEK1) is critical and sufficient for the activation of MMP-2. *Exp. Cell Res.* **254,** 180–188
60. Sudbeck, B. D., Baumann, P., Ryan, G. J., Breitkopf, K., Nischt, R., Krieg, T., and Mauch, C. (1999) Selective loss of PMA-stimulated expression of matrix metalloproteinase 1 in HaCaT keratinocytes is correlated with the inability to induce mitogen-activated protein family kinases. *Biochem. J.* **339,** 167–175
61. Shearer, T., and Crosson, C. E. (2001) Activation of extracellular signal-regulated kinase in trabecular meshwork cells. *Exp. Eye Res.* **73,** 25–35
62. Alvarado, J., Murphy, C., Polansky, J., and Juster, R. (1981) Age-related changes in trabecular meshwork cellularity. *Invest. Ophthalmol. Vis. Sci.* **21,** 714–727
63. Keating, A. (2012) Mesenchymal stromal cells: new directions. *Cell Stem Cell* **10,** 709–716
64. Pittenger, M. F., Mackay, A. M., Beck, S. C., Jaiswal, R. K., Douglas, R., Mosca, J. D., Moorman, M. A., Simonetti, D. W., Craig, S., and Marshak, D. R. (1999) Multilineage potential of adult human mesenchymal stem cells. *Science* **284,** 143–147
65. Caplan, A. I., and Dennis, J. E. (2006) Mesenchymal stem cells as trophic mediators. *J. Cell Biochem.* **98,** 1076–1084
66. Johnson, T. V., Dekorver, N. W., Levasseur, V. A., Osborne, A., Tassoni, A., Lorber, B., Heller, J. P., Villasmil, R., Bull, N. D., Martin, K. R., and Tomarev, S. I. (2014) Identification of retinal ganglion cell neuroprotection conferred by platelet-derived growth factor through analysis of the mesenchymal stem cell secretome. *Brain* **137,** 503–519
67. Kandyba, E., Leung, Y., Chen, Y. B., Widelitz, R., Chuong, C. M., and Kobielak, K. (2013) Competitive balance of intrabulge BMP/Wnt signaling reveals a robust gene network ruling stem cell homeostasis and cyclic activation. *Proc. Natl. Acad. Sci. U.S.A.* **110,** 1351–1356
68. Boquest, A. C., Shahdadfar, A., Frønsdal, K., Sigurjonsson, O., Tunheim, S. H., Collas, P., and Brinchmann, J. E. (2005) Isolation and transcription profiling of purified uncultured human stromal stem cells: alteration of gene expression after in vitro cell culture. *Mol. Biol. Cell* **16,** 1131–1141
69. van der Flier, L. G., van Gijn, M. E., Hatzis, P., Kujala, P., Haegebarth, A., Stange, D. E., Begthel, H., van den Born, M., Guryev, V., Oving, I., van Es, J. H., Barker, N., Peters, P. J., van de Wetering, M., and Clevers, H. (2009) Transcription factor achaete scute-like 2 controls intestinal stem cell fate. *Cell* **136,** 903–912
70. van der Flier, L. G., Haegebarth, A., Stange, D. E., van de Wetering, M., and Clevers, H. (2009) OLFM4 is a robust marker for stem cells in human intestine and marks a subset of colorectal cancer cells. *Gastroenterology* **137,** 15–17
71. Zhang, X., Huang, Q., Yang, Z., Li, Y., and Li, C. Y. (2004) GW112, a novel antiapoptotic protein that promotes tumor growth. *Cancer Res.* **64,** 2474–2481
72. Kim, K. K., Park, K. S., Song, S. B., and Kim, K. E. (2010) Up regulation of GW112 Gene by NF κB promotes an antiapoptotic property in gastric cancer cells. *Mol. Carcinog.* **49,** 259–270
73. Koshida, S., Kobayashi, D., Moriai, R., Tsuji, N., and Watanabe, N. (2007) Specific overexpression of OLFM4(GW112/HGC-1) mRNA in colon, breast and lung cancer tissues detected using quantitative analysis. *Cancer Sci.* **98,** 315–320
74. Aung, P. P., Oue, N., Mitani, Y., Nakayama, H., Yoshida, K., Noguchi, T., Bosserhoff, A. K., and Yasui, W. (2006) Systematic search for gastric cancer-specific genes based on SAGE data: melanoma inhibitory activity and matrix metalloproteinase-10 are novel prognostic factors in patients with gastric cancer. *Oncogene* **25,** 2546–2557
75. Marimuthu, A., Chavan, S., Sathe, G., Sahasrabuddhe, N. A., Srikanth, S. M., Renuse, S., Ahmad, S., Radhakrishnan, A., Barbhuiya, M. A., Kumar, R. V., Harsha, H. C., Sidransky, D., Califano, J., Pandey, A., and Chatterjee, A. (2013) Identification of head and neck squamous cell carcinoma biomarker candidates through proteomic analysis of cancer cell secretome. *Biochim. Biophys. Acta* **1834,** 2308–2316
76. Miljkovic-Licina, M., Hammel, P., Garrido-Urbani, S., Lee, B. P., Meguenani, M., Chaabane, C., Bochaton-Piallat, M. L., and Imhof, B. A. (2012) Targeting olfactomedin-like 3 inhibits tumor growth by impairing angiogenesis and pericyte coverage. *Mol. Cancer Ther.* **11,** 2588–2599